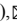


Review on the plastic instability of medium-Mn steels for identifying the formation mechanisms of Lüders and Portevin–Le Chatelier bands

Bin Hu¹,, Han Sui¹, Qinghua Wen¹, Zheng Wang¹, Alexander Gramlich², and Haiwen Luo¹,

1) School of Metallurgical and Ecological Engineering, University of Science and Technology Beijing, Beijing 100083, China

2) Steel Institute, RWTH Aachen University, Intzestraße 1, 52072 Aachen, Germany

(Received: 8 May 2023; revised: 24 September 2023; accepted: 25 September 2023)

Abstract: Plastic instability, including both the discontinuous yielding and stress serrations, has been frequently observed during the tensile deformation of medium-Mn steels (MMnS) and has been intensively studied in recent years. Unfortunately, research results are controversial, and no consensus has been achieved regarding the topic. Here, we first summarize all the possible factors that affect the yielding and flow stress serrations in MMnS, including the morphology and stability of austenite, the feature of the phase interface, and the deformation parameters. Then, we propose a universal mechanism to explain the conflicting experimental results. We conclude that the discontinuous yielding can be attributed to the lack of mobile dislocation before deformation and the rapid dislocation multiplication at the beginning of plastic deformation. Meanwhile, the results show that the stress serrations are formed due to the pinning and depinning between dislocations and interstitial atoms in austenite. Strain-induced martensitic transformation, influenced by the mechanical stability of austenite grain and deformation parameters, should not be the intrinsic cause of plastic instability. However, it can intensify or weaken the discontinuous yielding and the stress serrations by affecting the mobility and density of dislocations, as well as the interaction between the interstitial atoms and dislocations in austenite grains.

Keywords: medium manganese steel; discontinuous yielding; stress serrations; retained austenite; dislocations

1. Introduction

Medium-Mn (4wt%–12wt%) steels (MMnS), which are typically composed of ferrite, austenite, martensite, and even carbides, have attracted increasing attention due to their excellent comprehensive mechanical properties that benefit from the transformation-induced martensite transformation (TRIP) of metastable austenite [1–2]. In recent years, several processing routes have been proposed to generate some unusual microstructures in MMnS, resulting in unprecedented mechanical performance. For example, ultimate tensile strength (UTS) of 1.8 GPa and total elongation (TE) of 18% were achieved when austenite grains were tailored into different sizes and morphologies by a warm rolling process, resulting in enhanced strain hardening capability due to greater sustainable TRIP effect [3–4]. Moreover, the deformation and partition process was employed to generate high-density mobile dislocations in MMnS, leading to an ultrahigh yield strength (YS) of 2.2 GPa, TE of 16%, and fracture toughness of 101 MPa·m^{0.5} [5–6]. An ultrafast heating process was used to form the chemical boundaries in low-carbon medium-Mn steel, which improved UTS and TE to 2.3 GPa and 17%, respectively [7]. Very recently, multiple strengthening and plasticizing micro-mechanisms could be activated simultaneously in a deliberately designed hierarchical microstructure

consisting of laminated and twofold topologically aligned martensite and finely dispersed retained austenite (RA), resulting in UTS of higher than 2.2 GPa and TE of larger than 20% [8].

These ultrastrong MMnSs have promising applications in automobiles and armored and military instruments. However, they often exhibit some degree of plastic instability during tensile deformation, including the nucleation and propagation of Lüders and Portevin–Le Chatelier (PLC) bands [9–10], thus causing serious surface problems. The discontinuous yielding followed by three types of PLC bands, which are distinguished by the different serration patterns in the tensile flow curves, is schematically shown in Fig. 1 [11]. Type A bands are initiated at a certain location (often at a specimen extremity) and continuously propagated. Type B bands propagate by hopping along the longitudinal direction, whereas Type C bands are static bands that manifest in a spatially noncorrelated manner.

As these bands propagate locally, they lead to problematic surface roughening and, eventually, to the structural weakening of the material. Numerous studies have attempted to clarify the mechanisms of the discontinuous yielding and stress serrations in MMnS. Unfortunately, many of these have yielded controversial results, and none has been universally accepted to date. In this work, we systematically review experi-

 Corresponding authors: Bin Hu E-mail: hubin@ustb.edu.cn; Haiwen Luo E-mail: luohaiwen@ustb.edu.cn

© University of Science and Technology Beijing 2024

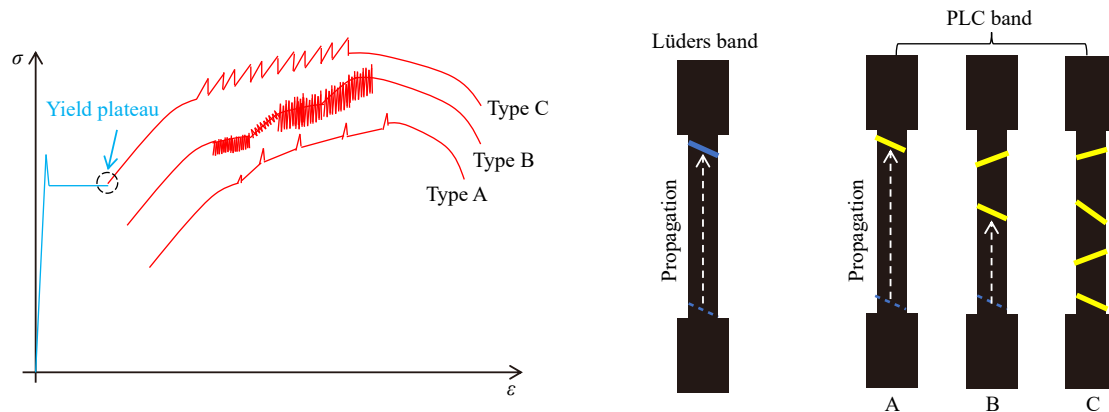


Fig. 1. Schematic diagram for yield plateau and different types of stress serrations in the stress–strain (σ – ϵ) curve, and the corresponding propagation of the Lüders band and different types of PLC bands.

mental results regarding the influence of discontinuous yielding and flow stress serrations during the tensile deformation of MMnS, including the metastable RA grains, the phase–interface configuration, and the deformation parameters, after which we discuss the possible mechanisms behind these influences. Next, we propose a universal explanation for the discontinuous yielding and stress serration phenomena of MMnS. Finally, we present a novel method of suppressing the plastic instability of MMnS and improving its mechanical properties before providing directions for future studies on the plastic instability of MMnS.

2. Discontinuous yielding mechanism in medium-Mn steels

2.1. Factors that affect yielding

2.1.1. Cottrell atmosphere formed in ferrite

Discontinuous yielding in plain carbon steel is related to the Cottrell atmosphere, which can lock mobile dislocations and unlock them under the upper yield point [12]. Therefore, by assuming that ferrite is relatively soft and determines the yielding behavior, the Lüders phenomenon in MMnS was initially believed to be influenced by interactions of interstitial atoms and dislocations in ferrite [13]. This mechanism can explain why both higher intercritical annealing (IA) temperature and longer IA duration could result in lower yield drop and shorter yield point elongation (YPE). This is because they both lead to a smaller fraction of ferrite formed with lower C concentration due to the enhanced partition of solute C from ferrite to austenite [14]. However, subsequent studies have reported that some MMnSs could exhibit discontinuous yielding even when austenite was softer than ferrite [15]. Moreover, this mechanism is unable to explain why the completely different yielding behaviors are observed in the MMnSs having the same fraction of ferrite but different grain morphologies (e.g., the lamellar or equiaxed austenite (γ) and ferrite (α) grains) [16].

2.1.2. Influence of retained austenite

(1) Mechanical stability of RA grains.

Since the austenite-to-martensite transformation at the Lüders front was first discovered [17], the relationship

between the yielding behavior and austenite stability has received increasing attention. Ryu *et al.* [18] concluded that the slower austenite transformation kinetics led to larger Lüders strain due to smaller work-hardening increments resulting from the TRIP effect. Ma *et al.* [19] found the Lüders band could be eliminated via stress-induced martensitic transformation before the initiation of plastic deformation, concluding that the lower stability of RA should favor the shorter YPE.

However, some contradictory observations have also been reported. For example, Zhang and Ding [20] proposed that the austenite-to-martensite transformation at the Lüders front increased the propagation distance of the Lüders band on the gauge section, leading to a larger YPE. Li *et al.* [21] found that pre-straining led to higher stability among the RA and a decreased Lüders strain during the tensile test. Using the advanced technique of high-speed digital image correlation (DIC), Wang *et al.* [22–23] monitored the microstructural evolution during the formation of Lüders bands. They noticed that the local strain increased more rapidly as the Lüders bands were nucleated. Comparing tensile deformation at 25 to 150°C (Fig. 2), it was found that TRIP could not occur in the latter case. Thus, it can be concluded that the martensitic transformation was not the cause of discontinuous yielding, although it accelerated the formation of the Lüders band by generating more dislocations. Moreover, the findings revealed that this phenomenon could lead to either the decrease of YPE as the high-strain hardening rate resulting from this transformation accelerates band propagation or to the increase of YPE when the specimen was fractured before the completion of propagation [24–27].

(2) Morphology of austenite and ferrite grains.

It has been widely reported that the discontinuous and continuous yielding of MMnS originated in the equiaxed and lamellar grain morphologies, respectively [16]. Han *et al.* [28] attributed the discontinuous yielding of MMnSs having equiaxed grains to the preferential yielding in the equiaxed ferrite, while the deformation of the lamellar austenite and ferrite grains took place simultaneously and compatibly, leading to continuous yielding. However, this mechanism was not supported by recent studies. For example, Dutta *et al.* [29] proposed that the lamellar austenite grains that inclined

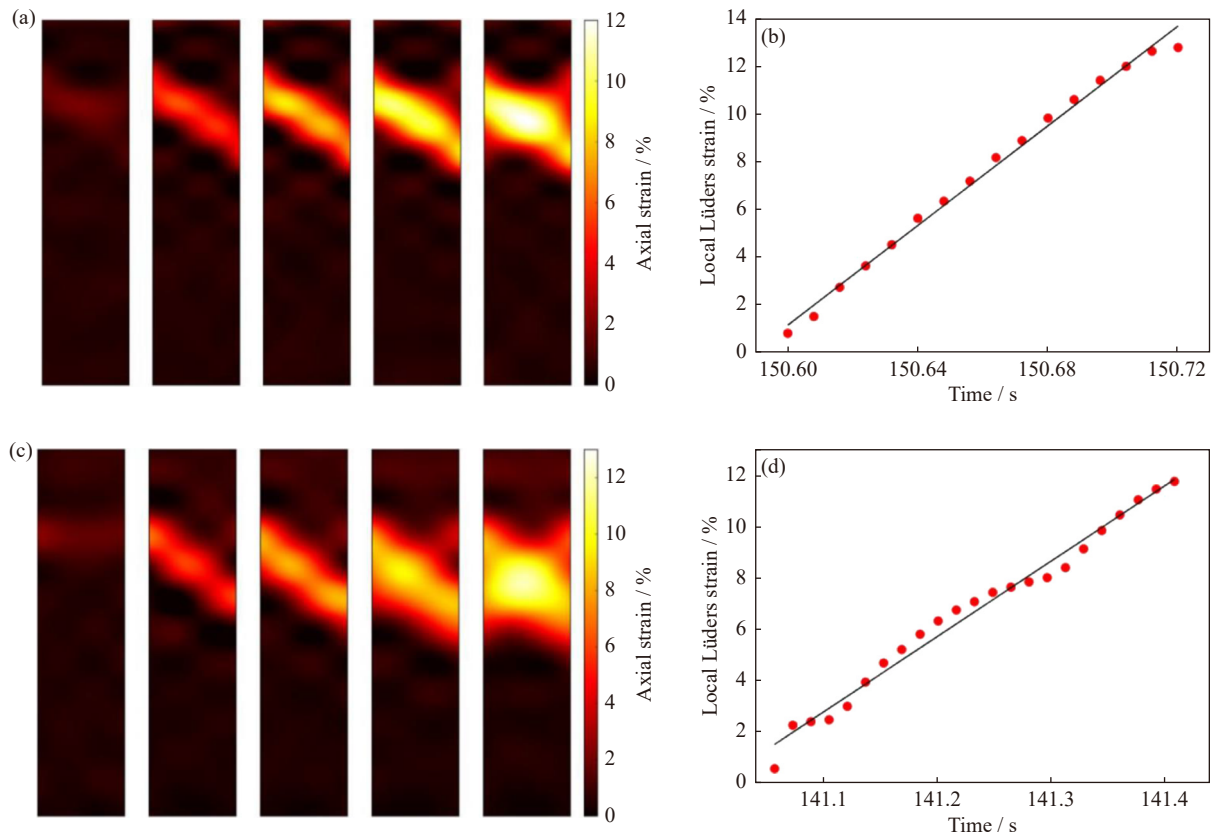


Fig. 2. Strain field measurement results of MMnS deformed at 25°C (a, b) and 150°C (c, d): (a, c) a succession of axial strain fields at the selected moments during the Lüders band formation; (b, d) evolution of the local Lüders strain with time during the Lüders band formation [22]. Reproduced from *Materialia*, 6, X.G. Wang, B.B. He, C.H. Liu, C. Jiang, and M.X. Huang, Extraordinary Lüders strain rate in medium-Mn steels, 100288, Copyright 2019, with permission from Elsevier.

by 45° to the loading axis were easily deformed and transformed to martensite, thus contributing to initial strain hardening and continuous yielding. Steineder *et al.* [30] found that the dislocation multiplication in lamellar microstructures was more pronounced than in the equiaxed morphologies. Therefore, they proposed that the higher dislocation interactions and accommodation capability in the lamellar microstructures caused continuous yielding. However, Sun *et al.* [31] suggested that stress concentration could easily build up at the tips of lamellar structures, thus leading to dislocations emitting effortlessly from the lamellar γ/α phase boundaries. This phenomenon resulted in dislocation multiplication at the initial plastic deformation and contributes to continuous yielding. Although the higher dislocation multiplication capacity in the lamellar grains has been reported in many studies, a widely accepted explanation remains lacking.

Furthermore, the lamellar and equiaxed grain morphologies usually result from the IA of hot- and cold-rolled microstructures, respectively [32]. The two types of microstructures differ not only in terms of grain morphologies but also in terms of the initial dislocation density and the extent of solute partitions between the two phases [33], in which the two latter factors may influence the yielding of MMnS. In this case, we have attempted to introduce ferrite and austenite grains with both the lamellar and equiaxed morphologies in one specimen via the austenitization-quenching IA process [34]. The results indicate that the lamellar and equiaxed

ferrite/austenite interfaces exhibit semicoherent and incoherent configurations. As a result, stacking faults and dislocations are easily emitted onto the interfaces of lamellar ferrite and austenite (Fig. 3(a)–(d)). The increased lamellar grains lead to larger microplasticity and more significant stress concentration on their neighboring equiaxed grains. In turn, this can result in dislocations emitted from the equiaxed ferrite/austenite interfaces, a phenomenon that occurs simultaneously with the equiaxed austenite-to-martensite transformation. Therefore, the increase in the volume fraction of lamellar grains results in a lower yield drop and shorter YPE.

2.1.3. Phase-interface configuration

To confirm the above-stated influences of austenite grains on yielding, Sun *et al.* [31] used advanced *in situ* techniques to characterize the microstructural evolution of MMnS during deformation from the macro-down to nanoscopic scale (i.e., from ~1 mm to below 100 nm). They concluded that the submicron grain size results in a comparatively large total α/γ interface area, providing a high density of dislocation sources. In turn, this leads to a rapid dislocation multiplication at the upper yield point, which is considered the main cause of the discontinuous yielding in MMnS. Furthermore, they proposed that the segregation of carbon to the α/γ interfaces might increase the energy barrier for dislocation emission, thereby providing a favorable condition for plastic flow avalanches and discontinuous yielding.

Furthermore, we studied the influence of the cooling rate

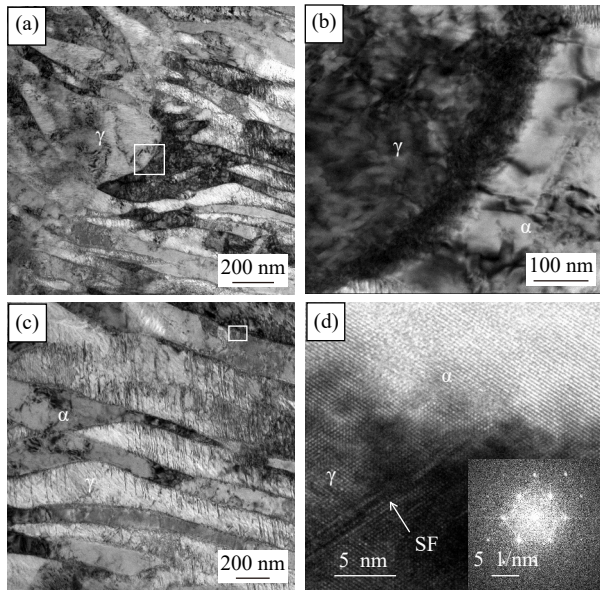


Fig. 3. Transmission electron microscope (TEM) examination on microstructures of one specimen having both equiaxed and lamellar microstructural morphologies after undergoing interrupted tensile tests at the end of yield plateau. As displayed, the density of emitted dislocations from the interface of equiaxed grains (a, b) is much lower than that for the semi-coherent interface of lamellar grains (c, d). (b) and (d) present the magnified view of areas marked by the white rectangles in (a) and (c); the corresponding fast fourier transformation (FFT) patterns is on the lower right corner of (d) [34]. Reprinted from *Materialia*, 20, B. Hu, F.L. Ding, X. Tu, *et al.*, Influence of lamellar and equiaxed microstructural morphologies on yielding behavior of a medium-Mn steel, 101252, Copyright 2021, with permission from Elsevier.

on the resulting phase-interface configuration and yielding behaviors of triplex MMnS. We also proposed that the high cooling rate during quenching favors geometry necessary

dislocations (GNDs) generated along the α'/α interface due to the more significant austenite-to-martensite transformation, which, in turn, contributes to continuous yielding (Fig. 4(a) and (b)). In comparison, lower cooling rates during air cooling from the same IA temperature allow for more C or Mn atoms to segregate to the α'/α interface (Fig. 4(c) and (d)), thereby leading to discontinuous yielding. At this point, the yield drops and YPE increases when the initial mobile dislocation density prior to deformation decreases due to either the reduced quantity of α'/α interfaces or the pinning of GNDs by the segregated C/Mn atoms along the interfaces [35–36].

2.1.4. Deformation temperature

Tensile deformation temperature also significantly influences the yielding behavior of MMnSs [37]. Zhang *et al.* [38] found that the YPE of a Fe–0.1%C–10%Mn–2%Al steel increased with the deformation temperature from –50 to 25°C but decreased from 25 to 100°C. Meanwhile, Wang and Huang [39] observed that the YPE had a nonmonotonic relationship with the deformation temperature when the MMnS was deformed in the range of 25–300°C, although few austenite grains transformed at the Lüders front at a higher temperature. Therefore, they attributed the increase of YPE to the longer dislocation slip distance during deformation. Discontinuous yielding even appeared in the stress–strain curves of cold-rolled MMnS during the deformation at 500°C because the grain size was still ultrafine (Fig. 5), but the further increase of deformation temperature led to grain coarsening and the transition to continuous yielding [40]. Therefore, the discontinuous yielding of MMnS appeared in a wide temperature range, but the YPE changed irregularly with deformation temperature.

2.2. Discontinuous yielding mechanism in MMnS

Among all the above-stated factors affecting the yielding

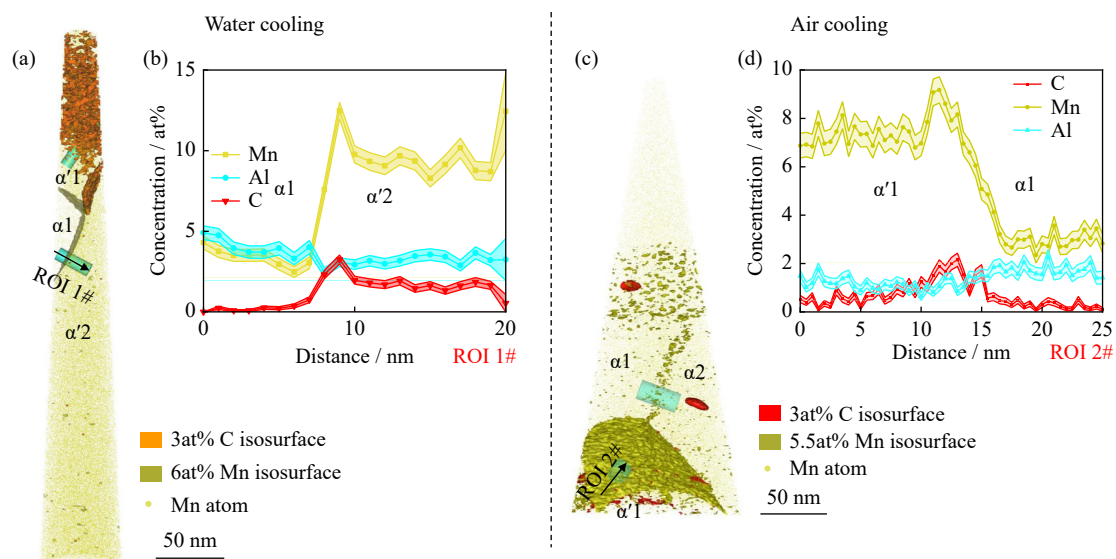


Fig. 4. (a, c) Manganese maps obtained by three-dimensional (3D) atom probe tomography in a 0.1C–5Mn–2Al steel that was water-cooled (a) and air-cooled (c) to room temperature after the same IA treatment; (b, d) concentration profiles across the phase and grain boundaries for C, Mn, and Al, which were taken from the selected regions of interest (ROI #1 and ROI #2) in (a) and (c) [36]. Reprinted from *J. Mater. Sci. Technol.*, 126, B. Hu, X. Shen, Q.Y. Guo, *et al.* Yielding behavior of triplex medium-Mn steel alternated with cooling strategies altering martensite/ferrite interfacial feature, 60–70, Copyright 2022, with permission from Elsevier.

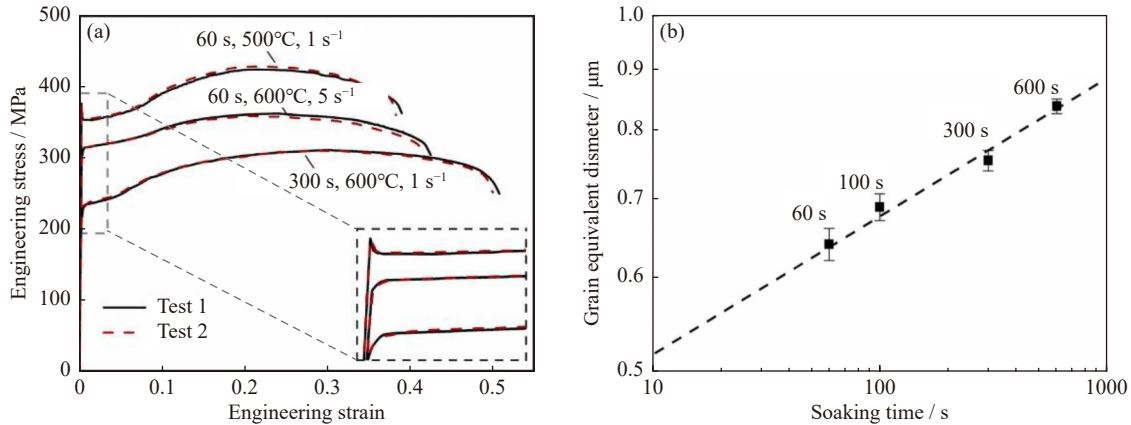


Fig. 5. (a) Flow curves for a cold-rolled 0.1C–8Mn–0.8Al steel under different deformation conditions; (b) average grain size of studied steel after austenitization at 780°C for different times [40]. Reproduced from *J Mater. Process Tech.*, 306, C.P. Tong, Q. Rong, V.A. Yardley, *et al.*, Investigation of deformation behavior with yield point phenomenon in cold-rolled medium-Mn steel under hot stamping conditions, 117623, Copyright 2022, with permission from Elsevier.

of MMnSs, the classical theory of the Cottrell atmosphere has failed to describe the influences of microstructural morphologies and deformation temperature on the yielding behavior. Thus, we proposed that the influence of all factors on yielding occurs by affecting the mobility and density of dislocations. In summary, discontinuous yielding results from several mobile dislocations available before deformation, but they can be rapidly multiplied with the plastic deformation, which represents the classical theory documented in the textbook [41] and is still applicable to date. For example, the influence of the phase-interface configuration on the yielding of MMnS is illustrated in Fig. 6(a)–(c). As can be seen, the lack of mobile dislocations along the γ/α interfaces before deformation and the rapid dislocation multiplication at the upper yield point led to discontinuous yielding of ferrite plus austenite duplex MMnS (Fig. 6(a)) [31]. The austenite-to-martensite transformation during quenching led to the GNDs generated along the α'/α interface in a triplex MMnS. This increased the mobile dislocation density before deformation and resulted in continuous yielding (Fig. 6(b)) [36]. In comparison, when the C/Mn solutes were segregated along the interfaces, the GNDs along the α'/α interface were locked, leading to discontinuous yielding (Fig. 6(c)) [31–36].

The influence of grain morphologies on the yielding of MMnS can be unified based on our previous study [34]. This phenomenon can be attributed to their different phase-interface configurations responsible for the different dislocation emission abilities and resultant yielding behaviors. The relationships among dislocation emission, the lamellar/equiaxed phase interface, and the mechanic response during the nucleation of Lüders bands in MMnS having both lamellar and equiaxed grains are schematically shown in Fig. 7(a)–(c), respectively. Many more dislocations are generated and multiplied in the lamellar grains at the initiation of plastic deformation because the stacking faults or dislocations are more easily emitted on the semicoherent lamellar ferrite/austenite interfaces than those on the incoherent equiaxed ferrite/austenite interfaces. This results in larger microplasticity and more significant stress concentration on their neighboring equiaxed

grains, in which some mobile dislocations are generated along the equiaxed ferrite/austenite interface as the mechanical response, along with the equiaxed austenite-to-martensite transformation and macro-yielding. Here, the values of yield drop and YPE gradually decreases with the increase in the fraction of lamellar grains because more mobile dislocations are generated along the lamellar ferrite/austenite grains with the semicoherent phase interface before macro-yielding.

This theory also has the potential to explain current controversial findings about the influences of austenite stability and deformation parameters on yielding behaviors, as discussed below. The Lüders band is formed at the limited overall plastic strain, but the local strain in the band can be large, and the one in front depends on the austenite fraction transformed, which can vary within the range of 5%–66% [4,42]. Therefore, austenite stability can also influence the yielding behaviors of MMnS [18–20]. Ma *et al.* [43] found that the austenite-to-martensite transformation at the Lüders front can be divided into two stages. Most transformations occur in the first half range, and almost no transformation occurs afterward. However, the Lüders band propagates continuously without interruption, indicating that the austenite-to-martensite transformation does not directly provide strain hardening for Lüders band propagation.

Recently, a hybrid measurement with *in situ* neutron diffraction and DIC was performed to evaluate the individual contribution of the austenite matrix and the deformation-induced martensite transformation to strain hardening during the Lüders band propagation [44]. This quantitative analysis revealed that the strain hardening required for the Lüders band to propagate is mostly provided by the formation of martensite [45–46]. The austenite-to-martensite transformation is accompanied by about 2%–4% volume change, generating residual stresses and producing GNDs in ferrite close to the ferrite/martensite interface [47–48].

Kadkhodapour *et al.* [49] calculated GND densities using the electron backscattered diffraction (EBSD) kernel average misorientation method and found that GND densities close to

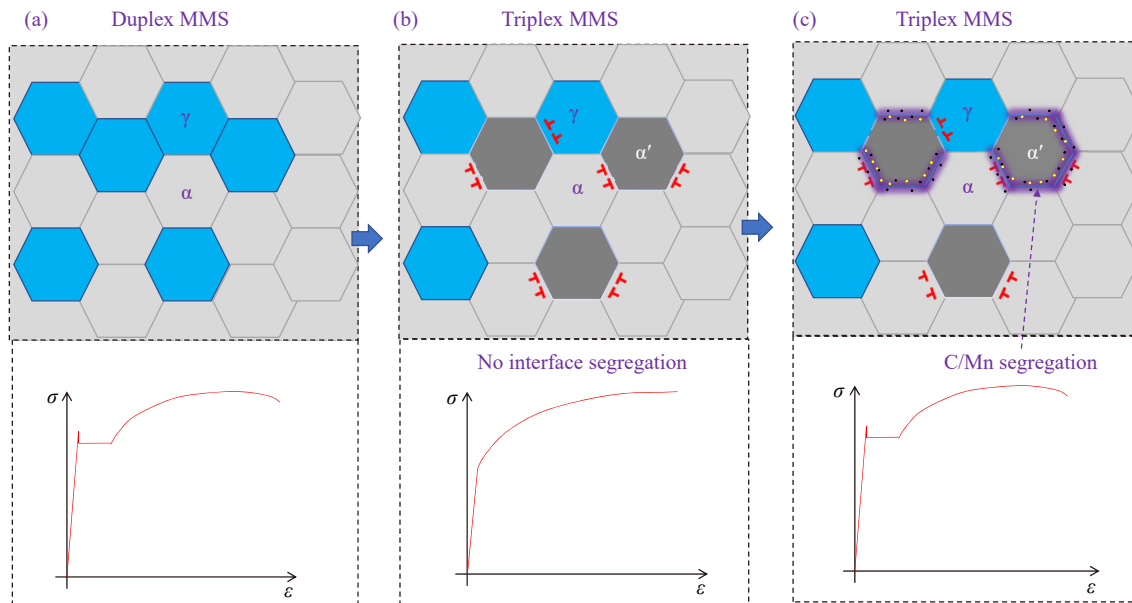


Fig. 6. Schematic illustrations showing the influence of the generation of GNDs and C/Mn segregation along the interface on the yielding behaviors of MMnS [36]. Reprinted from *J. Mater. Sci. Technol.*, 126, B. Hu, X. Shen, Q.Y. Guo, *et al.* Yielding behavior of triplex medium-Mn steel alternated with cooling strategies altering martensite/ferrite interfacial feature, 60–70, Copyright 2022, with permission from Elsevier.

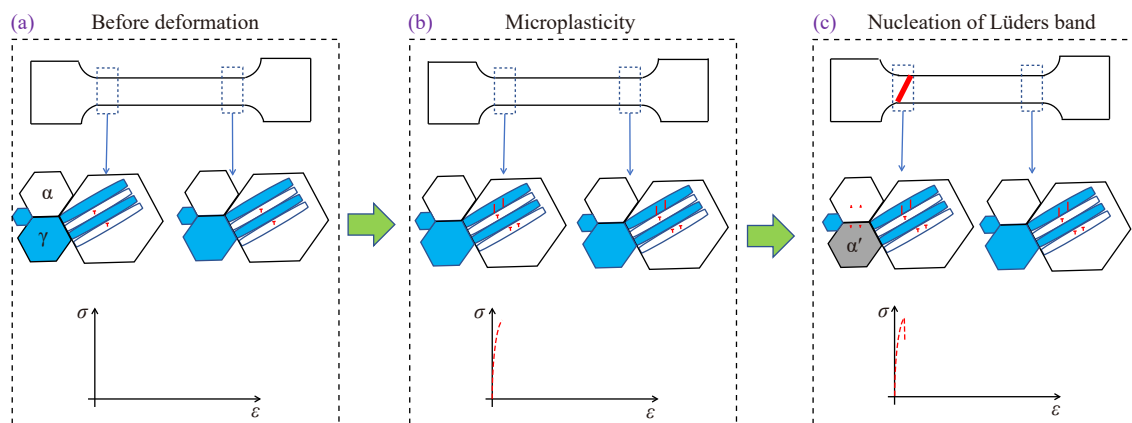


Fig. 7. Schematic illustrations of the Lüders bands' nucleation in MMnS comprising equiaxed plus lamellar microstructures, the corresponding microstructure evolution, and the changes in stress–strain curve [34]. Reprinted from *Materialia*, 20, B. Hu, F.L. Ding, X. Tu, *et al.*, Influence of lamellar and equiaxed microstructural morphologies on yielding behavior of a medium-Mn steel, 101252, Copyright 2021, with permission from Elsevier.

the ferrite–martensite interface is about $2.5 \times 10^{14} \text{ m}^{-2}$, which is one order higher than that away from the interface. Another study reported that austenite-to-martensite transformation should indirectly influence the strain hardening at the Lüders front by generating GNDs near the interface [43]. Consequently, the influence of austenite stability on the yielding behaviors can be explained as follows. The lower stability of austenite promotes more martensite formation with the increasing quantity of mobile GNDs. The slip of these mobile dislocations contributes to the initial strain hardening at low stresses. Thus, the stress-induced martensitic transformation contributes to continuous yielding [17]. However, when the RA grains are too fine to transform during the Lüders band propagation, the lack of mobile dislocation at the Lüders front may lead to premature fracture before the end of the yield plateau. For this reason, the lower stability of austenite

sometimes leads to a larger YPE value [20]. The prestrain leads to the RA with higher stability remaining, while the increase of dislocation density before the tensile test contributes to higher initial strain hardening and continuous yielding [21]. Therefore, these controversial experimental results on the influence of RA stability on discontinuous yielding behavior can be explained satisfactorily by the dislocation theory summarized above.

The YPE value of MMnS varies with deformation temperatures and can be attributed to grain size, dynamic recovery, and recrystallization [37–42,50–51]. However, these are also due to their influences on the density and mobility of dislocations. The ultrafine grain size remaining during deformation at 500°C may provide sufficient dislocation sources that, in turn, accelerate the dislocation multiplication at the upper yield point due to the large α/γ interface area, thus leading to

a significant yield drop [41]. Nevertheless, the deformation temperature influences the dislocations in many aspects, including the critical stress for dislocation slip, dislocation multiplication and annihilation due to the dynamic recovery, and the extent of solute segregation on dislocations. Consequently, the values of yield drop and YPE change irregularly with the deformation temperature [38–39].

3. PLC bands and flow stress serrations phenomenon

3.1. Factors influencing stress serrations

3.1.1. TRIP effect resulting from RA grains

The deformation-induced martensitic transformation is generally regarded as the cause of stress serrations in MMnSs due to the competition of the strengthening and softening effects of austenite-to-martensite transformation [52]. However, stress serrations often appear in high-Mn austenitic steels, even when there is no austenite transformed during the tensile test [53]. Sun *et al.* [54] observed the discontinuous strain-induced martensitic transformation (SIMT) at the PLC front in the MMnS by *in situ* magnetic induction measurements along with *ex situ* X-ray diffraction (XRD) examination. They found that the stress serrations only appeared in MMnS when the mechanical stability of austenite was mod-

erate. The decrease of austenite stability initially leads to a reduction of the critical strain necessary for activating PLC, such that the critical strain increases again if the austenite stability is further reduced [55]. However, Wang *et al.* [56] observed the presence of intensive stress serrations even though no austenite was transformed. Therefore, the austenite-to-martensite transformation should not be the intrinsic cause of stress serrations but can influence the nucleation and propagation of PLC bands. For instance, Yang *et al.* [57] investigated the deformation behavior of a 0.3C–7Mn–2Al MMnS. They demonstrated that PLC bands were subjected to a dynamic hindrance caused by the inside-band transformed martensite during propagation. In this case, the RA stability affected the dynamical formation of martensite and the properties of the PLC bands. Moderate austenite stabilities led to a rather small fraction of in-band transformed martensite, blocking the continuous movement of PLC bands. In turn, this resulted in Type A PLC bands, as illustrated in Fig. 8(a)–(c). On the contrary, RA with low stabilities can lead to large fractions of in-band transformed martensite, which means that the PLC band cannot easily overcome the resistance. Therefore, it might nucleate on other regions that have not been swept by the band, leading to the formation of Type A+B PLC bands, as schematically shown in Fig. 8(d)–(f).

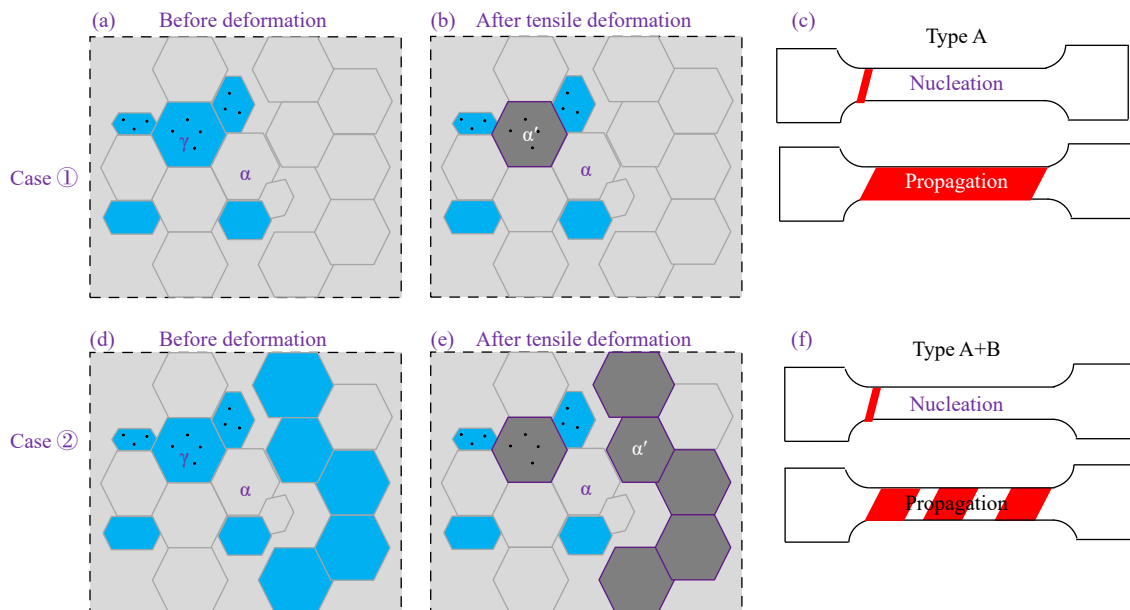


Fig. 8. Schematic diagram of how the influence of RA stability affects the types of PLC bands.

3.1.2. Tensile deformation parameters

The occurrence of the PLC band takes place in a specific temperature range, as the deformation temperature drastically influences the critical strain for activating the PLC effect. In particular, Min *et al.* [58] reported that the critical strain for activating the PLC effect increased with the decreasing deformation temperature. However, Grzegorzczuk *et al.* [59] concluded that the critical strains of 0.16C–4.7Mn–1.6Al–0.22Si–0.20Mo steel during deformation at 100 and 140°C were higher than that at 60°C. Moreover, it was found

that PLC serration occurred at larger strains or disappeared when deformed at higher temperatures, which can be attributed to the high temperatures facilitating carbon diffusion [60].

Recently, we found that stress serrations in a cold-rolled and annealed steel (0.29C–9Mn–2.4Al) could be fully removed when the deformation temperatures increased to 100 and 200°C (Fig. 9(a)). This can be attributed to more significant dynamic recoveries and SIMT being suppressed during deformation at high temperatures, which lead to signific-

ant decreases in the strain hardening rate (Fig. 9(a)–(e)). Moreover, the disappearance of PLC bands during deformation at temperatures higher than 200°C may be due to carbide precipitation. For example, Kipelova *et al.* [61] found that serrations disappeared due to the carbide precipitation at the deformation temperature of 350°C, thus reducing the concentrations of interstitial solutes.

Aside from the high deformation temperature, the occurrence of PLC bands can be suppressed by the increase in strain rate due to the generated adiabatic heat, leading to the increased diffusivity of interstitial atoms in turn [62]. However, the slower austenite-to-martensite transformation speed at the high-strain rate decreases the strain hardening rate, thus leading to negative strain hardening rate sensitivity and lower UTS [63].

3.2. Mechanism on flow stress serrations

Stress serrations that appear on the stress–strain curves of metallic materials are a thermal activation process, which is known to be caused by dynamic strain aging (DSA) [64]. The DSA phenomenon is usually observed in the 1st-generation advanced high strength steel in the high deformation temperature range of 150–650°C [65–67]. Strain aging in mild steel has been linked to the migration of carbon in solution toward dislocation cores, thus forming Cottrell atmospheres [68]. Zhou *et al.* [69] proposed that DSA in high-Cr alloyed ferritic steel was also caused by the diffusion of C atoms and by the pinning between C and moving dislocation, whereas the solute Cr had minimal influence on stress serrations. Choudhary *et al.* [70] studied the serrated yielding in a 9Cr–1Mo ferritic steel and found that the carbide precipitation reduced

the solute C concentration, resulting in the decrease in the serrations magnitude and an increase in the critical strain for the onset of serrations. Aside from ferritic steel, the stress serrations also appeared in the ferrite plus martensite double phased (DP) steel in the temperature range of 150–350°C and at low strain rates [71]. Queiroz *et al.* [72] reported that the calculated activation energy values for the beginning of the PLC effect and the maximum flow stress at 5% strain in DP steel corresponded to the activation energy for the carbon diffusion in ferrite and the energy for the carbon-dislocation interaction. This finding suggests that the DSA in DP steel occurs solely through the locking of dislocations by C atoms in ferrite, whereas the formation of carbide precipitation in martensite does not interfere with the DSA process. The high deformation temperature promotes the C diffusion toward dislocations, thus leading to dislocations inner ferrite easily move dragging their solute atmospheres. As a result, the DSA in DP steel and ferritic steels both appear at temperatures higher than 150°C.

Nevertheless, the nucleation and propagation of PLC bands are often observed at the beginning of plastic deformation in high-Mn (17wt%–30wt% Mn) twinning-induced plasticity (TWIP) steels and MMnSs at room temperature [73–74]. Our previous study on a 0.1C–5Mn steel consisting of ferrite and austenite showed that the strain localization in austenite led to the apparent stress serrations at the beginning of plastic deformation, which eventually disappeared after all RA grains transformed to martensite [75]. This indicates that the nucleation of PLC bands should be related to the plastic deformation of austenite, like in high-Mn steels.

Moreover, as shown in Fig. 9, the stress serrations in

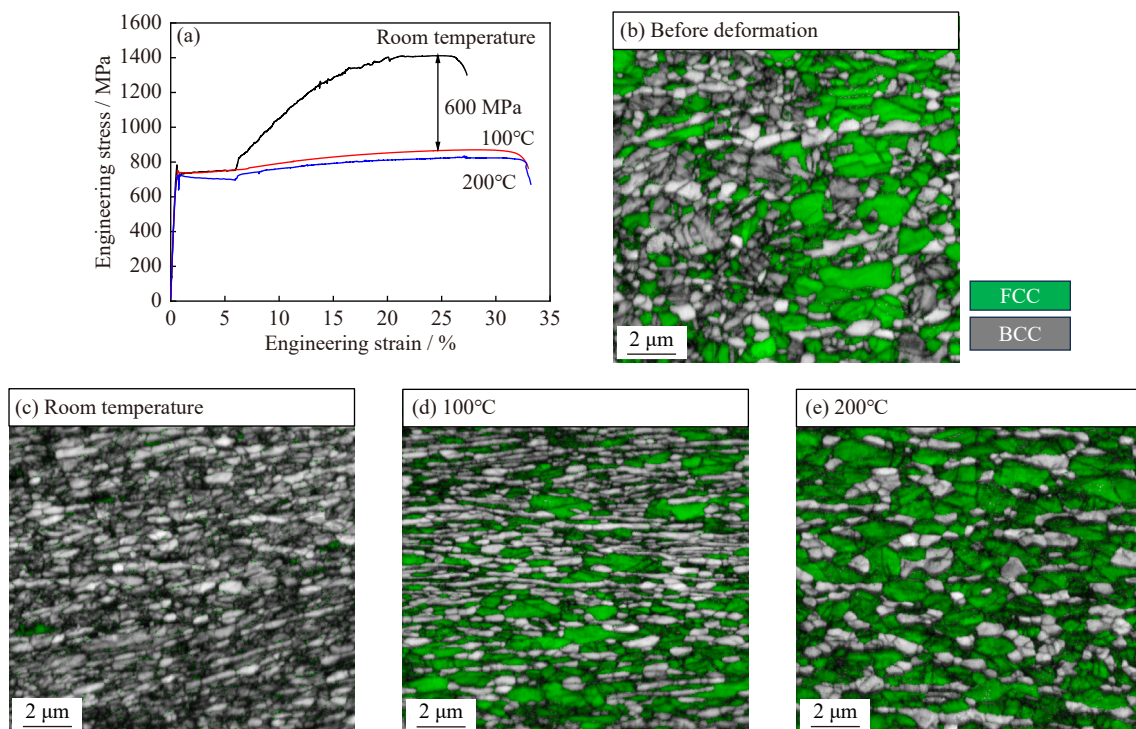


Fig. 9. Tensile properties and microstructures of a cold-rolled 0.29C–9Mn–2.4Al steel when deformed at different temperatures: (a) stress–strain curves of studied steel at different temperatures; (b–e) EBSD band contrast phase distribution map before deformation (b) and after tensile fracture at (c) room temperature, (d) 100°C, and (e) 200°C.

MMnS were significantly suppressed as the deformation temperatures increased from room temperature to 100 and 200°C. This result is highly different from that in ferritic and DP steel, although there are also some ultrafine ferrite grains in the MMnS similar to that in DP steel. The high deformation temperature in MMnS promotes the partition of C from the ferrite to the austenite phase, which then leads to the decreased C concentration in ferrite. Furthermore, the high deformation temperature promotes dynamic recovery and suppresses SIMT despite the fact that the C content in austenite is high. Both decrease the dislocation multiplication rate in austenite, leading to the disappearance of stress serrations.

The PLC band formation mechanism in high-Mn steel can be explained by the interaction between the solute atoms and dislocations, which is influenced by the stacking fault energy (SFE) of austenite. Lee *et al.* [76] proposed that DSA in high-Mn steels occurred due to the single diffusive jump of the interstitial C atoms of the C–Mn complex in the stacking faults region. Furthermore, they reported that the DSA only appeared when the residence time of the stacking fault at the location of the point defect complex was larger than the C reorientation time. This can explain why the addition of Al and N can suppress the DSA effect because it increases the SFE [77–78]. In addition, the decrease of C content in high-Mn steel can reduce the number of C–Mn complexes, resulting in the disappearance of stress serrations [79]. However, MMnS are less prone to the occurrence of PLC than high-Mn steels because the lower Mn content leads to higher SFE [80], while the much finer grain size in MMnS suppresses the dislocation multiplication within grains [81].

Dislocations are multiplied slowly in fine-grained austenite, which means that their quantity may be insufficient to induce the PLC band formation [82]. Furthermore, due to lower Mn concentration, the austenite grains in MMnS are more likely to transform to martensite than those in high-Mn steels. The influence of SIMT on stress serrations should also be attributed to its influence on dislocations. Recently, Sun *et al.* [83] have suggested that the martensite formed within the operating slip bands during deformation can locally block mobile dislocations and simultaneously change the status of C atoms to a more mobile and super-saturated state. In turn, this could make them rapidly move to the martensite–austenite interface. As a result, such C segregation can pin the dislocation sources at the hetero-interfaces, thereby increasing the critical stress required to emit new dislocations. The pinning effect of C atoms on the mobile dislocations along the interface has been observed by atom probe tomography (APT) examination in Fig. 4 [36].

In summary, the flow stress serrations in MMnS are caused by the pinning and depinning interaction between dislocation and the interstitial atoms in austenite, regardless of whether there is SIMT. The influence of SIMT and deformation parameters on the stress serrations is due to their varying impacts on the mobility and density of dislocation as well as the concentration and diffusion of solute C in austenite grains, all of which can influence the interaction between the

solute C atoms and dislocations.

Notably, Nam *et al.* [84] has indicated that the formation mechanism of Type A PLC serration in MMnS is related to the long-range pipe diffusion of C atoms instead of the reorientation of C–Mn complexes. This is different from the C diffusion mechanism in high-Mn TWIP steel and requires further investigation in the future.

4. Methods of suppressing the plastic instability of MMnS

The available studies on suppressing the plastic instability of MMnS mainly focus on regulating the thermomechanical processes and the tensile deformation parameters [85–87]. Here, the mechanical properties are often sacrificed simultaneously, although discontinuous yielding and stress serrations might be suppressed by decreasing the mechanical stability of RA or by raising the deformation temperature. In this case, it is necessary to find a novel pathway that could simultaneously suppress the plastic instability and enhance mechanical performance.

The electrical pulse process has been widely used to improve the tensile properties of metallic materials as an instantaneous high-energy input method. Furthermore, it was reported that electric pulse loading could suppress the PLC phenomenon in Al–Mg alloys due to its influence on dislocation movement and atom diffusion [88]. In comparison, Yi *et al.* [89] found that the pulsed electric current (PEC) suppressed the PLC effect as expected but with a significant strain hardening rate and UTS due to Joule heat generation. Nevertheless, we found that the PEC treatment before the tensile deformation strongly promoted martensite transformation, thus influencing the microstructures obtained by the quenching and partitioning process when the generated Joule heat was insufficient to facilitate reverse transformation during the PEC treatment [90]. The resulting microstructure is greatly refined, enhancing the mechanical stability and increasing GND generation near the α/α' and α'/α interfaces. Consequently, the resulting specimens yielded lower stress and achieved higher work-hardening rates as well as UTS, whereas the plastic strain localization, including the Lüders and PLC bands, were both strongly suppressed [91], as seen in Fig. 10(a)–(c).

5. Summarize and prospective

MMnS represents an emerging steel class currently being tapped for large-scale industrial implementation. While the combination of high strength and high ductility allows lightweight construction that increases the circularity of the produced components [92–94], the complex processes during plastic deformation must be fully understood to prevent problems during production or applications.

After conducting a systematic review of the factors governing the plastic instability of MMnS and analyzing the existing relevant mechanisms, we summarize that the discon-

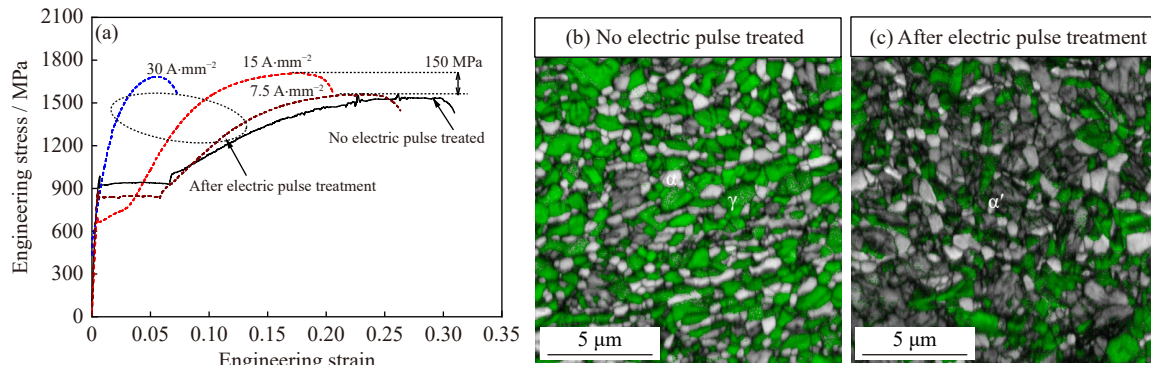


Fig. 10. Influence of electric pulse treatment on the tensile properties and microstructures of a 0.35C-9Mn-2Al cold-rolled and annealed steel: (a) Electric pulse treatment suppressed the stress serrations and enhanced strain hardening capacity; (b, c) EBSD band contrast overlapped by phase distribution images showing the microstructures before (b) and after (c) electric pulse treatment, the green in (b) and (c) represent austenite [90]. Reprinted from *Scripta Materialia*, 221, B. Hu, Q.H. Wen, Q.Y. Guo, Y.J. Wang, H. Sui, and H.W. Luo, A novel electric pulse pathway to suppress plastic localization and enhance strain hardening of medium-Mn steel, 114991, Copyright 2022, with permission from Elsevier.

tinuous yielding in MMnS can be attributed to the low density of mobile dislocations available before deformation, followed by the rapid multiplication at the upper yield point. Therefore, the discontinuous yielding of MMnS can be effectively suppressed by increasing mobile dislocations, which can be achieved by decreasing the austenite stability, pre-staining, and raising the cooling rate. Discontinuous yielding can also be achieved by inducing slower dislocation multiplication via the reduction of the total interface area. The stress serrations in MMnS can be attributed to the pinning and depinning interactions between dislocations and the interstitial atoms in austenite grains and can also be influenced by the RA stability. Therefore, the refinement of austenite grain and the lower C/Mn contents of austenite both suppress the occurrence of stress serrations in MMnS. However, the diffusive mechanism of C atoms in austenite during the tensile test remains unclear, thus requiring further investigations.

The current studies on discontinuous yielding and PLC stress serration formation mechanisms provide significant guidance in microstructure design that can suppress plastic instability. In particular, it has been demonstrated that the electric pulse-induced quenching and partitioning treatment can effectively suppress plastic instability and enhance the tensile properties of MMnS simultaneously. However, the mechanism of pulsed current-induced martensitic transformation is not yet well understood and requires further research. In addition, other thermomechanical processes that can assist the austenite-to-martensite transformation and refine RA grains must be explored because they are expected to have the same influence as the PEC treatment.

Future studies on the exact mechanisms of plastic instability can be extended to other research topics on MMnS. For example, hydrogen embrittlement of MMnSs has also been shown to be related to the emission, slip, and multiplication of dislocations similar to plastic instability [95]. However, the hydrogen embrittlement mechanism has not yet been well understood [96]. At the same time, although the increase of hydrogen content in MMnS has been found to decrease YS,

the scientific mechanism behind this remains clear [97]. Moreover, the measured dependence of yielding behaviors on charged hydrogen content can help reveal the hydrogen embrittlement mechanism in MMnS, which deserves more research in the future.

Acknowledgements

Haiwen Luo and Bin Hu acknowledge the financial support from the National Natural Science Foundation of China (Nos. 51831002, 51904028, and 52233018), the Beijing Municipal Natural Science Foundation (No. 2242048), and the Fundamental Research Funds for the Central Universities, China (No. FRF-EYIT-23-08).

Conflict of Interest

Haiwen Luo is an editorial board member for this journal and was not involved in the editorial review or the decision to publish this article. All authors declare that they have no known competing financial interests or personal relationships that could have appeared to influence the work reported in this paper.

References

- [1] D.W. Suh and S.J. Kim, Medium Mn transformation-induced plasticity steels: Recent progress and challenges, *Scripta Mater.*, 126(2017), p. 63.
- [2] B. Hu, H.W. Luo, F. Yang, and H. Dong, Recent progress in medium-Mn steels made with new designing strategies, a review, *J. Mater. Sci. Technol.*, 33(2017), No. 12, p. 1457.
- [3] B. Hu, B.B. He, G.J. Cheng, H. Yen, M.X. Huang, and H.W. Luo, Super-high-strength and formable medium Mn steel manufactured by warm rolling process, *Acta Mater.*, 174(2019), p. 131.
- [4] B. Hu and H.W. Luo, A strong and ductile 7Mn steel manufactured by warm rolling and exhibiting both transformation and twinning induced plasticity, *J. Alloys Compd.*, 725(2017), p. 684.
- [5] B.B. He, B. Hu, H.W. Yen, *et al.*, High dislocation density-in-

- duced large ductility in deformed and partitioned steels, *Science*, 357(2017), No. 6355, p. 1029.
- [6] L. Liu, Q. Yu, Z. Wang, J. Ell, M.X. Huang, and R.O. Ritchie, Making ultrastrong steel tough by grain-boundary delamination, *Science*, 368(2020), No. 6497, p. 1347.
- [7] R. Ding, Y. Yao, B. Sun, et al., Chemical boundary engineering: A new route toward lean, ultrastrong yet ductile steels, *Sci. Adv.*, 6(2020), No. 13, art. No. eaay1430.
- [8] Y.J. Li, G. Yuan, L.L. Li, et al., Ductile 2-GPa steels with hierarchical substructure, *Science*, 379(2023), No. 6628, p. 168.
- [9] Z.J. Teng, H.R. Wu, S. Pramanik, K.P. Hoyer, M. Schaper, H.L. Zhang, C. Boller, and P. Starke, Characterization and analysis of plastic instability in an ultrafine-grained medium Mn TRIP steel, *Adv. Eng. Mater.*, 24(2022), No. 9, art. No. 2200022.
- [10] B. Hu, X. Tu, Y. Wang, H.W. Luo, and X.P. Mao, Recent progress and future research prospects on the plastic instability of medium-Mn steels: A review, *Chin. J. Eng.*, 42(2020), No. 1, p. 48.
- [11] E. Pink and A. Grinberg, Serrated flow in a ferritic stainless steel, *Mater. Sci. Eng.*, 51(1981), No. 1, p. 1.
- [12] D. Akama, N. Nakada, T. Tsuchiyama, S. Takaki, and A. Hironaka, Discontinuous yielding induced by the addition of nickel to interstitial-free steel, *Scripta Mater.*, 82(2014), p. 13.
- [13] Y.K. Lee and J. Han, Current opinion in medium manganese steel, *Mater. Sci. Technol.*, 31(2015), No. 7, p. 843.
- [14] H.W. Luo, H. Dong, and M.X. Huang, Effect of intercritical annealing on the Lüders strains of medium Mn transformation-induced plasticity steels, *Mater. Des.*, 83(2015), p. 42.
- [15] B.H. Sun, F. Fazeli, C. Scott, N. Brodusch, R. Gauvin, and S. Yue, The influence of silicon additions on the deformation behavior of austenite–ferrite duplex medium manganese steels, *Acta Mater.*, 148(2018), p. 249.
- [16] J. Han, S.H. Kang, S.J. Lee, and Y.K. Lee, Fabrication of bimodal-grained Al-free medium Mn steel by double intercritical annealing and its tensile properties, *J. Alloys Compd.*, 681(2016), p. 580.
- [17] B.H. Sun, F. Fazeli, C. Scott, et al., Microstructural characteristics and tensile behavior of medium manganese steels with different manganese additions, *Mater. Sci. Eng. A*, 729(2018), p. 496.
- [18] J.H. Ryu, J.I. Kim, H.S. Kim, C.S. Oh, H.K.D.H. Bhadeshia, and D.W. Suh, Austenite stability and heterogeneous deformation in fine-grained transformation-induced plasticity-assisted steel, *Scripta Mater.*, 68(2013), No. 12, p. 933.
- [19] J.W. Ma, Q. Lu, L. Sun, and Y. Shen, Two-step intercritical annealing to eliminate Lüders band in a strong and ductile medium Mn steel, *Metall. Mater. Trans. A*, 49(2018), No. 10, p. 4404.
- [20] Y. Zhang and H. Ding, Ultrafine also can be ductile: On the essence of Lüders band elongation in ultrafine-grained medium manganese steel, *Mater. Sci. Eng. A*, 733(2018), p. 220.
- [21] Z.C. Li, H. Ding, R.D.K. Misra, and Z.H. Cai, Deformation behavior in cold-rolled medium-manganese TRIP steel and effect of pre-strain on the Lüders bands, *Mater. Sci. Eng. A*, 679(2017), p. 230.
- [22] X.G. Wang, B.B. He, C.H. Liu, C. Jiang, and M.X. Huang, Extraordinary Lüders-strain-rate in medium Mn steels, *Materialia*, 6(2019), art. No. 100288.
- [23] X.G. Wang, C.H. Liu, B.B. He, C. Jiang, and M.X. Huang, Microscopic strain partitioning in Lüders band of an ultrafine-grained medium Mn steel, *Mater. Sci. Eng. A*, 761(2019), art. No. 138050.
- [24] Y. Dong, M. Qi, Y. Du, H.Y. Wu, X.H. Gao, and L.X. Du, Significance of retained austenite stability on yield point elongation phenomenon in a hot-rolled and intercritically annealed medium-Mn steel, *Steel Res. Int.*, 93(2022), No. 11, art. No. 2200400.
- [25] J.Y. Zhang, Y.B. Xu, D.T. Han, and Z.L. Tong, Improving yield strength and elongation combination by tailoring austenite characteristics and deformation mechanism in medium Mn steel, *Scripta Mater.*, 218(2022), art. No. 114790.
- [26] P.J. Gibbs, E. De Moor, M.J. Merwin, B. Clausen, J.G. Speer, and D.K. Matlock, Austenite stability effects on tensile behavior of manganese-enriched-austenite transformation-induced plasticity steel, *Metall. Mater. Trans. A*, 42(2011), No. 12, p. 3691.
- [27] I. Miyazaki, T. Furuta, K. Oh-ishi, et al., Overcoming the strength-ductility trade-off via the formation of a thermally stable and plastically unstable austenitic phase in cold-worked steel, *Mater. Sci. Eng. A*, 721(2018), p. 74.
- [28] J. Han, S.J. Lee, J.G. Jung, and Y.K. Lee, The effects of the initial martensite microstructure on the microstructure and tensile properties of intercritically annealed Fe–9Mn–0.05C steel, *Acta Mater.*, 78(2014), p. 369.
- [29] A. Dutta, D. Ponge, S. Sandlöbes, and D. Raabe, Strain partitioning and strain localization in medium manganese steels measured by *in situ* microscopic digital image correlation, *Materialia*, 5(2019), art. No. 100252.
- [30] K. Steineder, D. Krizan, R. Schneider, C. Béal, and C. Sommitsch, On the microstructural characteristics influencing the yielding behavior of ultra-fine grained medium-Mn steels, *Acta Mater.*, 139(2017), p. 39.
- [31] B.H. Sun, Y. Ma, N. Vanderesse, et al., Macroscopic to nanoscopic *in situ* investigation on yielding mechanisms in ultrafine grained medium Mn steels: Role of the austenite-ferrite interface, *Acta Mater.*, 178(2019), p. 10.
- [32] M.S. Jeong, T.M. Park, S. Choi, S.J. Lee, and J. Han, Recovering the ductility of medium-Mn steel by restoring the original microstructure, *Scripta Mater.*, 190(2021), p. 16.
- [33] T.W.J. Kwok and D. Dye, A review of the processing, microstructure and property relationships in medium Mn steels, *Int. Mater. Rev.*, 68(2023), No. 8, p. 1058.
- [34] B. Hu, F.L. Ding, X. Tu, et al., Influence of lamellar and equiaxed microstructural morphologies on yielding behaviour of a medium Mn steel, *Materialia*, 20(2021), art. No. 101252.
- [35] Y. Ma, B.H. Sun, A. Schökel, et al., Phase boundary segregation-induced strengthening and discontinuous yielding in ultrafine-grained duplex medium-Mn steels, *Acta Mater.*, 200(2020), p. 389.
- [36] B. Hu, X. Shen, Q.Y. Guo, et al., Yielding behavior of triplex medium Mn steel alternated with cooling strategies altering martensite/ferrite interfacial feature, *J. Mater. Sci. Technol.*, 126(2022), p. 60.
- [37] Y. Wang, M. Zhang, Q.Y. Cen, W.J. Wang, and X.Y. Sun, A novel process combining thermal deformation and intercritical annealing to enhance mechanical properties and avoid Lüders strain of Fe–0.2C–7Mn TRIP steel, *Mater. Sci. Eng. A*, 839(2022), art. No. 142849.
- [38] M.H. Zhang, L.F. Li, J. Ding, et al., Temperature-dependent micromechanical behavior of medium-Mn transformation-induced-plasticity steel studied by *in situ* synchrotron X-ray diffraction, *Acta Mater.*, 141(2017), p. 294.
- [39] X.G. Wang and M.X. Huang, Temperature dependence of Lüders strain and its correlation with martensitic transformation in a medium Mn transformation-induced plasticity steel, *J. Iron Steel Res. Int.*, 24(2017), No. 11, p. 1073.
- [40] C.P. Tong, Q. Rong, V.A. Yardley, et al., Investigation of deformation behaviour with yield point phenomenon in cold-rolled medium-Mn steel under hot stamping conditions, *J. Mater. Process. Technol.*, 306(2022), art. No. 117623.
- [41] D. Hull and D.J. Bacon, *Introduction to Dislocations*, 4th ed., Butterworth-Heinemann, Oxford, 2001, p. 214.
- [42] S. Gao, Y. Bai, R.X. Zheng, et al., Mechanism of huge Lüders-type deformation in ultrafine grained austenitic stainless steel,

- Scripta Mater.*, 159(2019), p. 28.
- [43] J.W. Ma, H.T. Liu, Q. Lu, Y. Zhong, L. Wang, and Y. Shen, Transformation kinetics of retained austenite in the tensile Lüders strain range in medium Mn steel, *Scripta Mater.*, 169(2019), p. 1.
- [44] W.Q. Mao, S. Gao, W. Gong, S. Harjo, T. Kawasaki, and N. Tsuji, Quantitatively evaluating the huge Lüders band deformation in an ultrafine grain stainless steel by combining *in situ* neutron diffraction and digital image correlation analysis, *Scripta Mater.*, 235(2023), art. No. 115642.
- [45] W.J. Yin, F. Briffod, H.Y. Hu, K. Yamazaki, T. Shiraiwa, and M. Enoki, Quantitative investigation of strain partitioning and failure mechanism in ultrafine grained medium Mn steel through high resolution digital image correlation, *Scripta Mater.*, 229(2023), art. No. 115386.
- [46] M. Çobanoğlu, R.K. Ertan, C. Şimşir, and M. Efe, Excessive damage increase in dual phase steels under high strain rates and temperatures, *Int. J. Damage Mech.*, 30(2021), No. 2, p. 283.
- [47] M. Calcagnotto, D. Ponge, E. Demir, and D. Raabe, Orientation gradients and geometrically necessary dislocations in ultrafine grained dual-phase steels studied by 2D and 3D EBSD, *Mater. Sci. Eng. A*, 527(2010), No. 10-11, p. 2738.
- [48] D.A. Korzekwa, D.K. Matlock, and G. Krauss, Dislocation substructure as a function of strain in a dual-phase steel, *Metall. Trans. A*, 15(1984), No. 6, p. 1221.
- [49] J. Kadkhodapour, S. Schmauder, D. Raabe, S. Ziaei-Rad, U. Weber, and M. Calcagnotto, Experimental and numerical study on geometrically necessary dislocations and non-homogeneous mechanical properties of the ferrite phase in dual phase steels, *Acta Mater.*, 59(2011), No. 11, p. 4387.
- [50] H.J. Pan, X.Y. Li, B. Qiao, *et al.*, A medium-Mn steel stamped parts overcoming Lüders deformation by increasing dislocation density, *J. Mater. Eng. Perform.*, 31(2022), No. 2, p. 1.
- [51] G.Q. Su, H.B. Xie, M.S. Huo, *et al.*, Yielding behavior and strengthening mechanisms of a high strength ultrafine-grained Cr–Mn–Ni–N stainless steel, *Steel Res. Int.*, 93(2022), No. 5, art. No. 2100524.
- [52] Z.H. Cai, H. Ding, R.D.K. Misra, and Z.Y. Ying, Austenite stability and deformation behavior in a cold-rolled transformation-induced plasticity steel with medium manganese content, *Acta Mater.*, 84(2015), p. 229.
- [53] M.H. Barati Rizi, M. Ghiasabadi Farahani, M. Aghaahmadi, J.H. Kim, L.P. Karjalainen, and P. Sahu, Analysis of strain hardening behavior of a high-Mn TWIP steel using electron microscopy and cyclic stress relaxation, *Acta Mater.*, 240(2022), art. No. 118309.
- [54] B.H. Sun, N. Vanderesse, F. Fazeli, *et al.*, Discontinuous strain-induced martensite transformation related to the Portevin–Le Chatelier effect in a medium manganese steel, *Scripta Mater.*, 133(2017), p. 9.
- [55] A. Müller, C. Segel, M. Linderov, A. Vinogradov, A. Weidner, and H. Biermann, The Portevin–Le Chatelier effect in a metastable austenitic stainless steel, *Metall. Mater. Trans. A*, 47(2016), No. 1, p. 59.
- [56] X.G. Wang, L. Wang, and M.X. Huang, Kinematic and thermal characteristics of Lüders and Portevin–Le Chatelier bands in a medium Mn transformation-induced plasticity steel, *Acta Mater.*, 124(2017), p. 17.
- [57] F. Yang, H.W. Luo, E.X. Pu, S.L. Zhang, and H. Dong, On the characteristics of Portevin–Le Chatelier bands in cold-rolled 7Mn steel showing transformation-induced plasticity, *Int. J. Plast.*, 103(2018), p. 188.
- [58] J.Y. Min, L.G. Hector Jr, L. Zhang, L. Sun, J.E. Carsley, and J.P. Lin, Plastic instability at elevated temperatures in a TRIP-assisted steel, *Mater. Des.*, 95(2016), p. 370.
- [59] B. Grzegorzczak, A. Kozłowska, M. Morawiec, R. Muszyński, and A. Grajcar, Effect of deformation temperature on the Portevin–Le Chatelier effect in medium-Mn steel, *Metals*, 9(2018), No. 1, art. No. 2.
- [60] P. Lan and J.Q. Zhang, Serrated flow and dynamic strain aging in Fe–Mn–C TWIP steel, *Metall. Mater. Trans. A*, 49(2018), No. 1, p. 147.
- [61] A. Kipelova, R. Kaibyshev, V. Skorobogatykh, and I. Schenkova, Portevin–Le Chatelier effect in an E911 creep resistant steel with 3%Co additives, *J. Phys. Conf. Ser.*, 240(2010), art. No. 012100.
- [62] A. Rusinek and J.R. Klepaczko, Experiments on heat generated during plastic deformation and stored energy for TRIP steels, *Mater. Des.*, 30(2009), No. 1, p. 35.
- [63] S. Sevssek, C. Haase, and W. Bleck, Strain-rate-dependent deformation behavior and mechanical properties of a multi-phase medium-manganese steel, *Metals*, 9(2019), No. 3, art. No. 344.
- [64] P. Rodriguez, Serrated plastic flow, *Bull. Mater. Sci.*, 6(1984), No. 4, p. 653.
- [65] B. M. Gonzalez, L. Marchi, E. J. Fonseca, P. J. Modenesi, and V. Buono, Measurement of dynamic strain aging in pearlitic steels by tensile test, *ISIJ Int.*, 43(2003), p. 428.
- [66] B. Bayramin, C. Şimşir, and M. Efe, Dynamic strain aging in DP steels at forming relevant strain rates and temperatures, *Mater. Sci. Eng. A*, 704(2017), p. 164.
- [67] M.J. Molaei and A. Ekrami, The effect of dynamic strain aging on subsequent mechanical properties of dual-phase steels, *J. Mater. Eng. Perform.*, 19(2010), No. 4, p. 607.
- [68] A.H. Cottrell and B.A. Bilby, Dislocation theory of yielding and strain ageing of iron, *Proc. Phys. Soc. A*, 62(1949), No. 1, p. 49.
- [69] H.W. Zhou, J.F. Fang, Y. Chen, *et al.*, Internal friction studies on dynamic strain aging in P91 ferritic steel, *Mater. Sci. Eng. A*, 676(2016), p. 361.
- [70] B.K. Choudhary, K. Bhanu Sankara Rao, S.L. Mannan, and B.P. Kashyap, Serrated yielding in 9Cr–1Mo ferritic steel, *Mater. Sci. Technol.*, 15(1999), No. 7, p. 791.
- [71] S. Chandran, W.Q. Liu, J.H. Lian, S. Münstermann, and P. Verleysen, Dynamic strain aging in DP1000: Effect of temperature and strain rate, *Mater. Sci. Eng. A*, 832(2022), art. No. 142509.
- [72] R.R.U. Queiroz, F.G.G. Cunha, and B.M. Gonzalez, Study of dynamic strain aging in dual phase steel, *Mater. Sci. Eng. A*, 543(2012), p. 84.
- [73] D.D. Li, L.H. Qian, C.Z. Wei, S. Liu, F.C. Zhang, and J.Y. Meng, The tensile properties and microstructure evolution of cold-rolled Fe–Mn–C TWIP steels with different carbon contents, *Mater. Sci. Eng. A*, 839(2022), art. No. 142862.
- [74] W. Bleck, New insights into the properties of high-manganese steel, *Int. J. Miner. Metall. Mater.*, 28(2021), No. 5, p. 782.
- [75] B. Hu and H.W. Luo, A novel two-step intercritical annealing process to improve mechanical properties of medium Mn steel, *Acta Mater.*, 176(2019), p. 250.
- [76] S.J. Lee, J. Kim, S.N. Kane, and B.C. De Cooman, On the origin of dynamic strain aging in twinning-induced plasticity steels, *Acta Mater.*, 59(2011), No. 17, p. 6809.
- [77] S. Lee, J. Kim, S.J. Lee, and B.C. De Cooman, Effect of nitrogen on the critical strain for dynamic strain aging in high-manganese twinning-induced plasticity steel, *Scripta Mater.*, 65(2011), No. 6, p. 528.
- [78] J.H. Kang, T. Ingendahl, J. von Appen, R. Dronskowski, and W. Bleck, Impact of short-range ordering on yield strength of high manganese austenitic steels, *Mater. Sci. Eng. A*, 614(2014), p. 122.
- [79] L. Bracke, J. Penning, and N. Akdut, The influence of Cr and N additions on the mechanical properties of FeMnC steels, *Metall. Mater. Trans. A*, 38(2007), No. 3, p. 520.
- [80] A. Grajcar, P. Skrzypczyk, and D. Wozniak, Thermomechanically rolled medium-Mn steels containing retained austenite/walcowane termomechanicznie stale średniomanganowe zawierające austenit szczątkowy, *Arch. Metall. Mater.*,

- 59(2014), No. 4, p. 1691.
- [81] D.M. Field and D.C. Van Aken, Dynamic strain aging phenomena and tensile response of medium-Mn TRIP steel, *Metall. Mater. Trans. A*, 49(2018), No. 4, p. 1152.
- [82] H.Y. Liu, S. Liu, C.Z. Wei, L.H. Qian, Y.L. Feng, and F.C. Zhang, Effect of grain size on dynamic strain aging behavior of C-bearing high Mn twinning-induced plasticity steel, *J. Mater. Res. Technol.*, 15(2021), p. 6387.
- [83] B.H. Sun, A. Kwiatkowski da Silva, Y.X. Wu, et al., Physical metallurgy of medium-Mn advanced high-strength steels, *Int. Mater. Rev.*, 68(2023), No. 7, p. 786.
- [84] J.H. Nam, S.K. Oh, M.H. Park, and Y.K. Lee, The mechanism of dynamic strain aging for type A serrations in tensile curves of a medium-Mn steel, *Acta Mater.*, 206(2021), art. No. 116613.
- [85] S.S. Li and H.W. Luo, Medium-Mn steels for hot forming application in the automotive industry, *Int. J. Miner. Metall. Mater.*, 28(2021), No. 5, p. 741.
- [86] P.Y. Wen, J.S. Han, H.W. Luo, and X.P. Mao, Effect of flash processing on recrystallization behavior and mechanical performance of cold-rolled IF steel, *Int. J. Miner. Metall. Mater.*, 27(2020), No. 9, p. 1234.
- [87] Y.J. Wang, S. Zhao, R.B. Song, and B. Hu, Hot ductility behavior of a Fe–0.3C–9Mn–2Al medium Mn steel, *Int. J. Miner. Metall. Mater.*, 28(2021), No. 3, p. 422.
- [88] H. Xu, X.B. Liu, D. Zhang, and X.F. Zhang, Minimizing serrated flow in Al–Mg alloys by electroplasticity, *J. Mater. Sci. Technol.*, 35(2019), No. 6, p. 1108.
- [89] K. Yi, S. Zhou, and X.F. Zhang, Suppression of serrated flow in medium Mn steel under pulsed electric current, *Mater. Sci. Eng. A*, 846(2022), art. No. 143271.
- [90] B. Hu, Q.H. Wen, Q.Y. Guo, Y.J. Wang, H. Sui, and H.W. Luo, A novel electric pulse pathway to suppress plastic localization and enhance strain hardening of medium Mn steel, *Scripta Mater.*, 221(2022), art. No. 114991.
- [91] B. Hu and H.W. Luo, *A Method and Process of Inhibiting the Local Plastic Instability of High/Medium Mn Steel*, Chinese Patent, Appl. 202011497048.X, 2022.
- [92] A. Gramlich, T. Schmiedl, S. Schönborn, T. Melz, and W. Bleck, Development of air-hardening martensitic forging steels, *Mater. Sci. Eng. A*, 784(2020), art. No. 139321.
- [93] A. Gramlich, W. Hagedorn, K. Greiff, and U. Krupp, Air cooling martensites—The future of carbon neutral steel forgings?, *Adv. Eng. Mater.*, 25(2023), No. 15, art. No. 2201931.
- [94] Z.J. Xie, C.J. Shang, X.L. Wang, X.M. Wang, G. Han, and R.D.K. Misra, Recent progress in third-generation low alloy steels developed under M³ microstructure control, *Int. J. Miner. Metall. Mater.*, 27(2020), No. 1, p. 1.
- [95] B.H. Sun, W. Krieger, M. Rohwerder, D. Ponge, and D. Raabe, Dependence of hydrogen embrittlement mechanisms on microstructure-driven hydrogen distribution in medium Mn steels, *Acta Mater.*, 183(2020), p. 313.
- [96] J. Han, J.H. Nam, and Y.K. Lee, The mechanism of hydrogen embrittlement in intercritically annealed medium Mn TRIP steel, *Acta Mater.*, 113(2016), p. 1.
- [97] L. Cho, Y.R. Kong, J.G. Speer, and K.O. Findley, Hydrogen embrittlement of medium Mn steels, *Metals*, 11(2021), No. 2, art. No. 358.